

Additive Manufacturing of Syntactic Foams: Part 1: Development, Properties, and Recycling Potential of Filaments

ASHISH KUMAR SINGH,¹ BALU PATIL,² NIKLAS HOFFMANN,³
BROOKS SALTONSTALL,¹ MRITYUNJAY DODDAMANI,²
and NIKHIL GUPTA^{1,4}

1.—Composite Materials and Mechanics Laboratory, Mechanical and Aerospace Engineering Department, Tandon School of Engineering, New York University, Brooklyn, NY 11201, USA. 2.—Advanced Manufacturing Laboratory, Department of Mechanical Engineering, National Institute of Technology Karnataka, Surathkal, India. 3.—Institut für Maschinenwesen, Technische Universität Clausthal, Clausthal-Zellerfeld, Germany. 4.—e-mail: ngupta@nyu.edu

This work focuses on developing filaments of high-density polyethylene (HDPE) and their hollow particle-filled syntactic foams for commercial three-dimensional (3D) printers based on fused filament fabrication technology. Hollow fly-ash cenospheres were blended by 40 wt.% in a HDPE matrix to produce syntactic foam (HDPE40) filaments. Further, the recycling potential was studied by pelletizing the filaments again to extrude twice (2×) and three times (3×). The filaments were tensile tested at 10^{-4} s^{-1} , 10^{-3} s^{-1} , and 10^{-2} s^{-1} strain rates. HDPE40 filaments show an increasing trend in modulus and strength with the strain rate. Higher density and modulus were noticed for 2× filaments compared to 1× filaments because of the crushing of some cenospheres in the extrusion cycle. However, 2× and 3× filament densities are nearly the same, showing potential for recycling them. The filaments show better properties than the same materials processed by conventional injection molding. Micro-CT scans show a uniform dispersion of cenospheres in all filaments.

INTRODUCTION

Additive manufacturing (AM) has become one of the fastest growing fields in recent years.^{1,2} Advances in AM have resulted in capabilities of producing complex functional parts on site at short lead times.³ The product development life cycle is considerably shortened with the use of AM methods that can produce parts even in small production runs.⁴ Components manufactured by AM are finding applications in automotive, aerospace, and medical fields, with several examples of in-service parts now available in these sectors.^{5,6}

Industry-standard size filaments of 1.75-mm or 3-mm diameter are commonly made for fused deposition modeling (FDM) printers from thermoplastics such as acrylonitrile butadiene styrene, polylactic acid, polyethylene terephthalate, or their blends.^{3,4}

Composites have become mainstream industrial materials in many applications, and their filaments are also being developed.^{7,8}

Syntactic foams are hollow particle-filled composite materials that are of great interest in weight-sensitive applications.^{9,10} Thermoplastic syntactic foam components have traditionally been manufactured by injection or compression molding.^{11,12} However, studies on AM of syntactic foams are not yet available mainly because of the challenges associated with manufacturing quality filaments, which include particle breakage during blending and filament extrusion. In addition, the process of three-dimensional (3D) printing can also lead to particle fracture, which needs to be minimized. An additional benefit of syntactic foam filaments is that the use of low-cost particulate fillers can lead to saving of matrix resin and make the filament cheaper than the filament of neat resin. Hence,

even if the hollow particle reinforcement does not provide benefit in properties in some cases, the low cost and saving of resin leading to greener filaments would be beneficial. While casting and machining of syntactic foams is possible, 3D printing provides greater flexibility in many existing applications. For example, an entire underwater vehicle structure, including internal details of instrumentation housings and buoyancy chambers, can be 3D printed without requiring any adhesives or fasteners.

Challenges of particle fracture, porosity entrapment, and incomplete mixing are involved in developing a cenosphere/HDPE syntactic foam filament, which are addressed in the present work. Further, the recycling potential of syntactic foam filaments is studied by pelletizing and extruding them twice (2×) and three times (3×). Success in recycling syntactic foam filaments would make them more environmentally friendly even after printing the objects and using them in some applications.

MATERIALS AND METHODS

Filament Material

HDPE of HD50MA180 grade is procured from Reliance Polymers, Mumbai, India, in the form of 3-mm-diameter granules of 97,500 g/mol mean molecular weight. Cenospheres (CIL-150 grade) are supplied by Cenospheres India Pvt. Ltd., Kolkata, India. Chemical and particle size analysis details of cenospheres are presented elsewhere.¹¹ Syntactic foams with 40 wt.% cenospheres are blended and are designated by HDPE40. In previous studies, the HDPE40 composition was found to be the highest filling level of cenospheres without substantial fracture.^{11,12}

Pellet Manufacturing and Filament Extrusion

HDPE40 is produced using Brabender (CMEI, MODEL-16 CME SPL, Western Company Keltron) and melted to form approximately $4 \times 4 \times 3 \text{ mm}^3$ pellets, which are fed into a laboratory-scale filament extruder having two heating zones. The extruder design is finalized based on the initial pilot experiments and quality of the filament. Two heaters are controlled separately using solid-state relays that are switched on/off by an Arduino using the input from two K-type thermocouples attached to each heater. The primary and secondary heaters are set at 127°C and 120°C, respectively. After preheating of HDPE40 pellets for 10 min, the material is extruded through a die with a 2.2-mm hole to obtain the 1× filament. The 1× filament is pelletized and fed into the hopper again to prepare the 2× filament, and the process is repeated one more time to obtain the 3× filament. At least five specimens are cut from random sections of each HDPE and HDPE40 filaments, and the mass and volume are measured to calculate the density.

Imaging

A Hitachi S-3400 N scanning electron microscope (SEM), equipped with backscattered and secondary electron detectors, is used to study the filament microstructure. Specimens are coated with gold using a Cressington 108 Auto Sputter Coater prior to imaging.

The internal structure of filaments is studied by using a Bruker Skyscan 1172 micro-CT scanner equipped with a digital x-ray camera having a 4000×2664 -pixel array (corresponding to 4 K resolution). The specimens are placed 36.55 mm and 308.36 mm from the source and camera, respectively, resulting in a pixel size of $0.95 \mu\text{m}$. A rotation step of 0.2° is used in scanning. Samples are exposed for 1420 ms at a source voltage of 50 kV.

Tensile testing

An Instron 4467 Universal Testing System with a 30-kN load cell is used to perform tensile tests at 10^{-4} s^{-1} , 10^{-3} s^{-1} , and 10^{-2} s^{-1} strain rates. A 1-inch gauge length Instron extensometer is used to measure strain. At least five specimens of each filament type at each strain rate are tested.

RESULTS AND DISCUSSION

Filament Quality and Density

HDPE40-2× and 3× filaments are observed to have a uniform cross-section in SEM observations. The average diameters of 2× and 3× filaments are measured to be $1.72 \pm 0.01 \text{ mm}$, suggesting extrusion consistency. The blended HDPE40 pellets and 1×, 2×, and 3× filaments have densities of $0.807 \pm 0.016 \text{ g/cm}^3$, $0.905 \pm 0.076 \text{ g/cm}^3$, $0.966 \pm 0.018 \text{ g/cm}^3$, and $0.975 \pm 0.022 \text{ g/cm}^3$, respectively. The theoretical density of HDPE40 pellets, estimated using the rule of mixtures, is 0.943 g/cm^3 . The density of the foam increases after each extrusion pass, although the values are in a small range. The standard deviation is higher for the HDPE40-1× filament, suggesting entrapment of voids and breakage of cenospheres during the extrusion process. The entrapped air porosity is expected to reduce with each pass, making the density more consistent. However, breakage of particles in each pass results in an increase in density and is undesirable. Due to the large standard deviation hinting at quality inconsistencies in the HDPE-1× filament, they are not subjected to tensile testing in this work.

Density of syntactic foams does not show any significant change between the second and the third extrusion pass. Since the density of the cenosphere wall material is around 3.5 g/cm^3 , stabilization of density below 1 g/cm^3 shows that there is no additional particle fracture or void entrapment.

Filament Microstructure

Figure 1a shows a low-magnification micrograph of the HDPE-1 \times filament. Cenospheres are observed to be uniformly distributed around the cross section of the filament. A close observation of the filament microstructure in Fig. 1b suggests some broken fragments among mostly intact cenospheres. Figure 1c and d shows the microstructure of the HDPE40-2 \times and 3 \times specimens. Since the density of HDPE40-2 \times and 3 \times filaments is the same, their microstructures also reflect that fact and appear to be very similar. The second and third extrusion passes under similar processing conditions do not lead to significant additional breakage of particles. This observation shows that the recycling of the syntactic foam filament is possible.

Figure 2a presents micro-CT 3D reconstruction of one representative HDPE40-1 \times specimen. The filament specimens are mounted with the length oriented along the z-axis. Cenospheres are observed to be uniformly distributed across all sections in the filament. There are a few limitations of the micro-CT scan analysis due to varying cenosphere wall thicknesses and wall porosities (Fig. 2b and c).

Figure 2d presents successive trans-axial images (i, ii, iii, and iv) that are 2-pixel distance apart. Highlighted regions “a” and “b” in Fig. 2d show defects on the cenosphere surface and wall porosities. The circles highlight a portion of the same cenosphere that appears to be broken in image (iii) and solid in image (iv). It is likely that this discontinuity is caused by one of the defects similar to those shown in Fig. 2b and c. Some of these defective regions may make the walls appear broken in an intact cenosphere in micro-CT images, which makes it difficult to obtain reliable results from image analysis. Such deviations lead to erroneous data, and thereby experimental density estimation to quantify hollow particle breakage is the relatively better approach in case of cenospheres.

Tensile Behavior

HDPE resin shows a ductile behavior with necking and plastic deformation. A similar deformation pattern for the HDPE-2 \times and 3 \times filaments is observed at all strain rates. In comparison, the failure mode of the HDPE40-2 \times and 3 \times filaments is observed to be brittle without any visible sign of

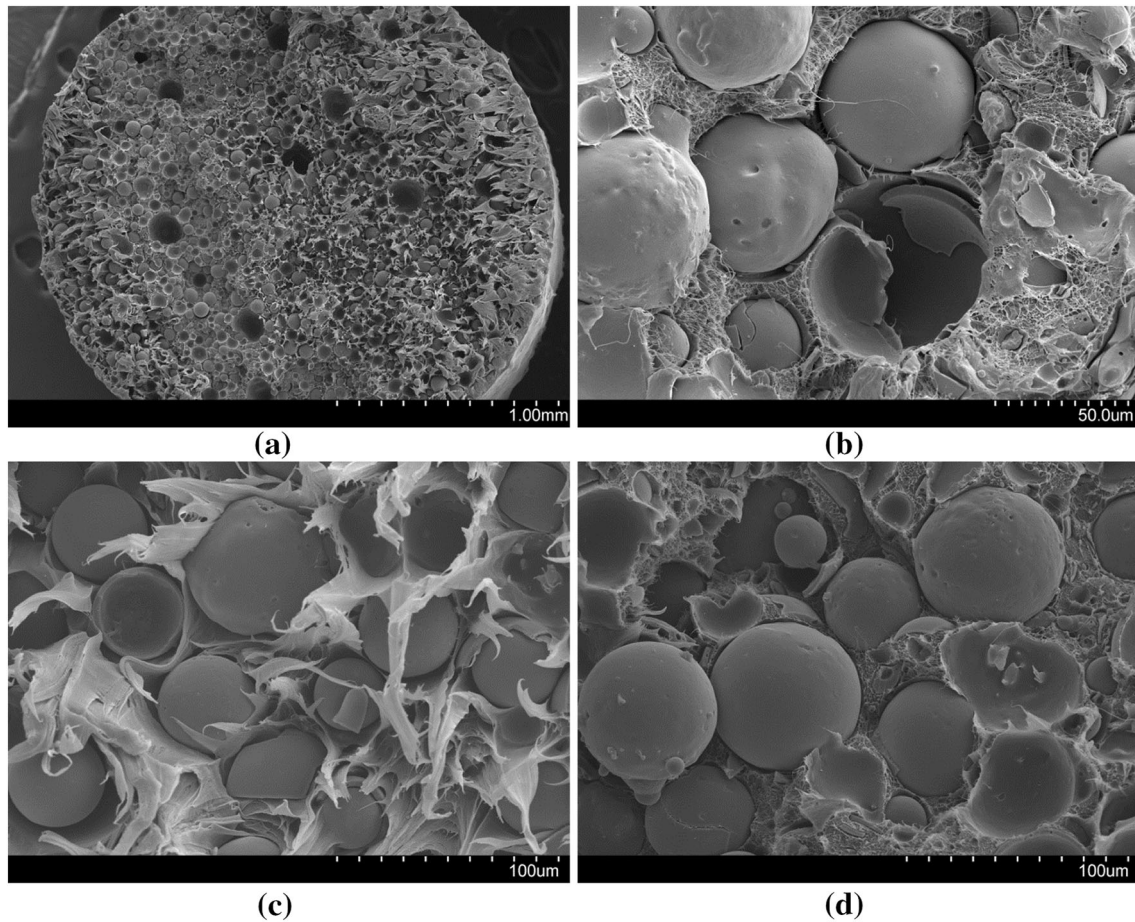


Fig. 1. Micrograph of (a) HDPE40-1 \times filament at low magnification; (b) a higher magnification image; and (c) HDPE40-2 \times and (d) HDPE40-3 \times filaments.

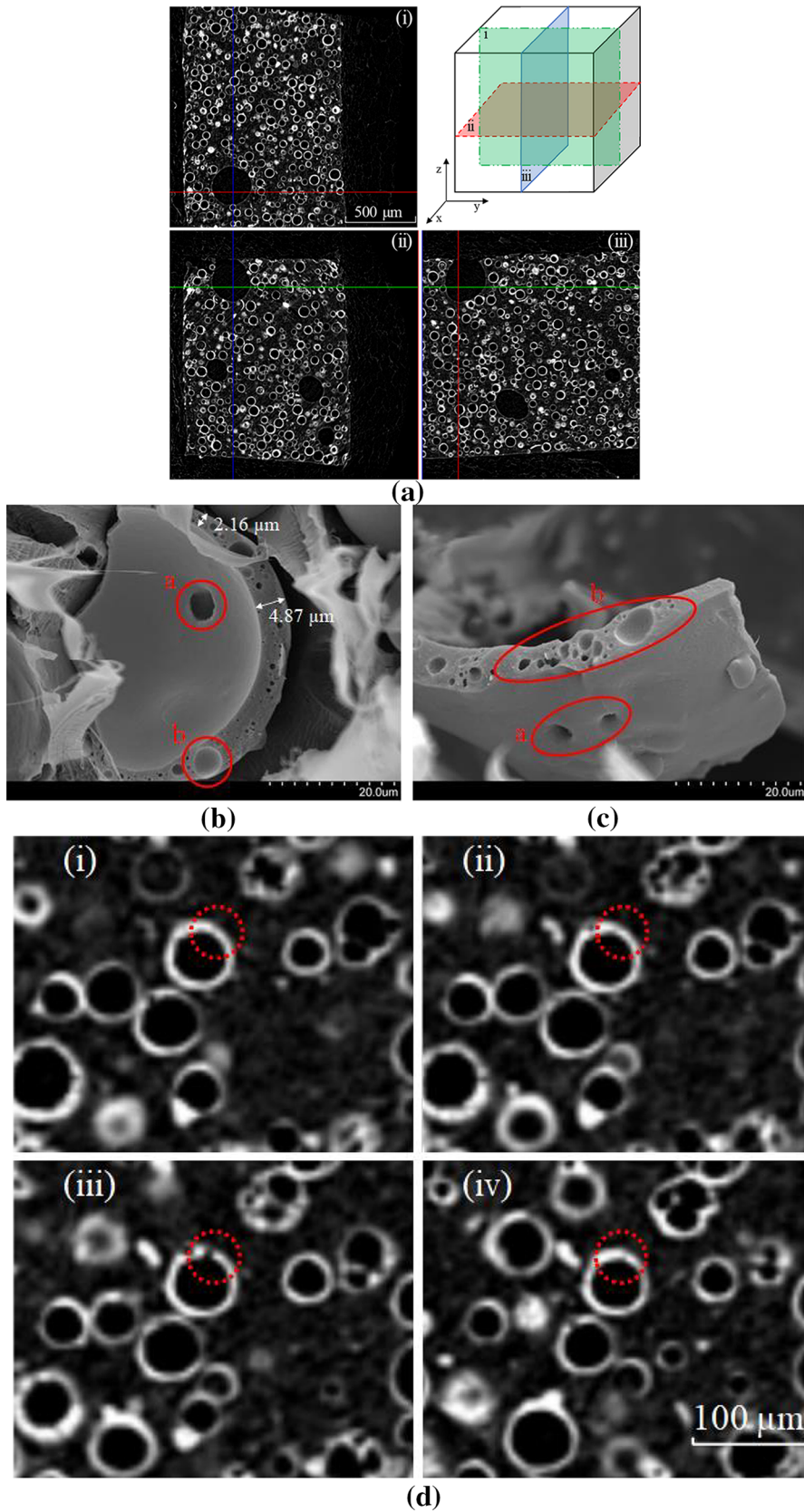


Fig. 2. (a) Micro-CT scan image showing reconstructed (i) sagittal (y-z), (ii) trans-axial (x-y), and (iii) coronal (z-x) views of the HDPE40-1x specimen, (b) and (c) micrographs showing cenosphere walls with porosities and variable thicknesses, and (d) voids present in the cenosphere walls can appear to be discontinuities in some slices in the micro-CT scan images of HDPE40.

Table I. Tensile properties of extruded HDPE and HDPE40 filaments

Filament	Strain rate (s^{-1})	Modulus (MPa)	Yield strength (MPa)	Ultimate tensile strength (MPa)
HDPE-1 \times	10^{-4}	353 ± 28	6.7 ± 1.5	11.5 ± 0.6
	10^{-3}	536 ± 26	8.0 ± 0.2	12.7 ± 0.9
	10^{-2}	687 ± 33	13.3 ± 0.7	16.1 ± 0.3
HDPE-2 \times	10^{-4}	380 ± 39	8.8 ± 0.8	14.6 ± 0.8
	10^{-3}	521 ± 10	10.0 ± 0.4	17.3 ± 0.6
	10^{-2}	719 ± 13	12.3 ± 0.3	20.3 ± 1.0
HDPE-3 \times	10^{-4}	397 ± 55	6.1 ± 1.7	13.9 ± 1.3
	10^{-3}	545 ± 70	10.3 ± 1.6	17.8 ± 0.9
	10^{-2}	732 ± 59	13.1 ± 1.2	21.0 ± 1.0
HDPE40-2 \times	10^{-4}	744 ± 71	7.2 ± 0.2	8.6 ± 0.3
	10^{-3}	897 ± 9	5.1 ± 0.2	8.0 ± 0.1
	10^{-2}	1020 ± 11	9.8 ± 0.4	11.7 ± 0.0
HDPE40-3 \times	10^{-4}	403 ± 83	5.6 ± 1.6	7.0 ± 0.8
	10^{-3}	620 ± 84	6.4 ± 0.6	8.8 ± 0.7
	10^{-2}	722 ± 11	6.9 ± 1.5	9.0 ± 1.3

necking, which is also observed in injection-molded syntactic foams.¹³ Inclusion of stiffer cenospheres in a relatively soft and compliant HDPE matrix leads to such a behavior.

Figure 3a, b, and c presents stress–strain plots for neat HDPE filaments at different strain rates. Most filaments fracture at a lower strain of 12–15% compared to the injection-molded ones (over 100% strain).¹³ The modulus and yield strength (0.2% strain offset method) values for HDPE filaments are listed in Table I. The modulus is 11%, 2%, and 6% higher for HDPE-3 \times filaments compared to HDPE-1 \times at strain rates of 10^{-4} , 10^{-3} , and 10^{-2} , respectively. Although this change is very small, the values are higher for all strain rates for filaments compared to the injection-molded specimens. HDPE extrusion cycles lead to alignment of polymer chains,¹⁴ resulting in an increase in yield strength and modulus. At the same time, thermal processing of HDPE leads to crosslinking in the individual polymer chains, increasing stiffness as reported previously by other groups.¹⁵ An increase in strain rate increases the filament modulus and strength. Ultimate tensile strength (UTS) values of the 1 \times , 2 \times , and 3 \times filaments at the same strain rates show an increasing trend, further backing the hardening process due to crosslinking.

A similar trend in the modulus with strain rate is noted for HDPE40-2 \times and 3 \times specimens (Fig. 3d and e; Table I). The only anomaly of this trend is observed in the yield strength and ultimate tensile strength of HDPE40-2 \times at $10^{-3} s^{-1}$, which shows lower values than $10^{-4} s^{-1}$ strain rates as observed in Fig. 3d. Nonetheless, given the trends of all other materials in this study, these one-test condition results are an anomaly. Since densities of both these filaments are about the same, a reduction in mechanical properties of HDPE40-3 \times is likely because of the orientation of broken fragments of cenospheres during the extrusion process, leading to failure due to stress concentration effects. Thin-

walled ceramic fragments have two orders of magnitude higher stiffness than the matrix resin and sharp edges, which can cause severe stress concentration effects at the interface and initiate cracks. The strength of syntactic foams in all extruded conditions is in a narrow range, which can be useful in 3D-printed components by making their properties more predictable and reliable.

Figure 3f summarizes the results of tensile behavior for HDPE40 processed by injection molding and filament extrusion methods. HDPE40-2 \times and 3 \times filaments show an increasing trend in the specific modulus with the strain rate. The specific modulus of HDPE40-3 \times filaments is similar to that of the injection-molded specimen.¹¹ The specific modulus is strongly influenced by the number of intact particles in the matrix during processing. The results suggest that the particle survival rate is similar in both processes.

Figure 4a and b presents tensile failure features in the HDPE40-2 \times filament at $10^{-4} s^{-1}$ strain rate. Plastic deformation of the HDPE matrix can be observed in the form of long fibrils. In addition, some broken and intact cenospheres are also observed in these micrographs. Due to extremely high failure strain in thermoplastic resins and poor interfacial bonding between the particle and matrix, the appearance of excessive plastic deformation of the matrix and relatively unaffected particles is common for such materials, which is also observed in studies related to injection-molded specimens.¹³

CONCLUSION

The present work is focused on developing HDPE and HDPE-fly ash cenosphere syntactic foams for use in commercial FDM 3D printers. It is highly desired to increase the available selection of filament materials for printing components that can be put into service directly after printing. The filament recyclability potential is also addressed.

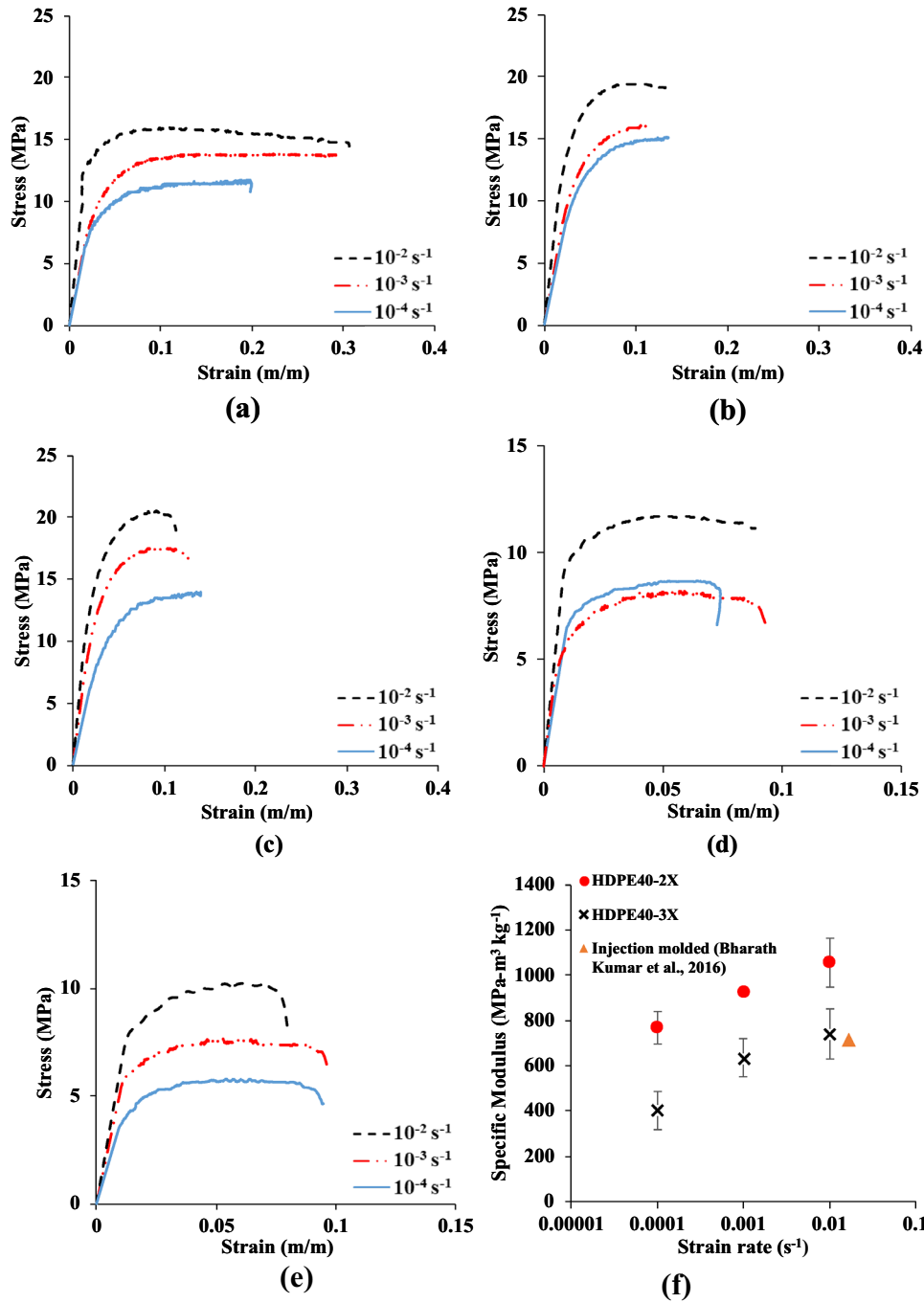


Fig. 3. Representative stress vs. strain curves for tensile behavior of (a) HDPE-1 \times , (b) HDPE-2 \times , (c) HDPE-3 \times , (d) HDPE40-2 \times , and (e) HDPE40-3 \times filaments. (f) The specific modulus versus strain rate plot for HDPE40 filaments versus injection-molded HDPE40.

- Density of HDPE40 foams increased in up to two extrusion passes because of cenosphere breakage and porosity consolidation.
- The tensile modulus and yield strength of neat HDPE filaments increased with each extrusion pass.
- HDPE40 filaments show an increasing trend in modulus and strength with strain rate. HDPE40 foams also show higher mechanical properties

than the HDPE specimens under comparable processing conditions.

- Specific modulus values of extruded filaments are higher than those of injection-molded samples at the same strain rates.

These results show that the developed filaments have potential to be used in 3D printing as the properties are comparable to the injection-molded

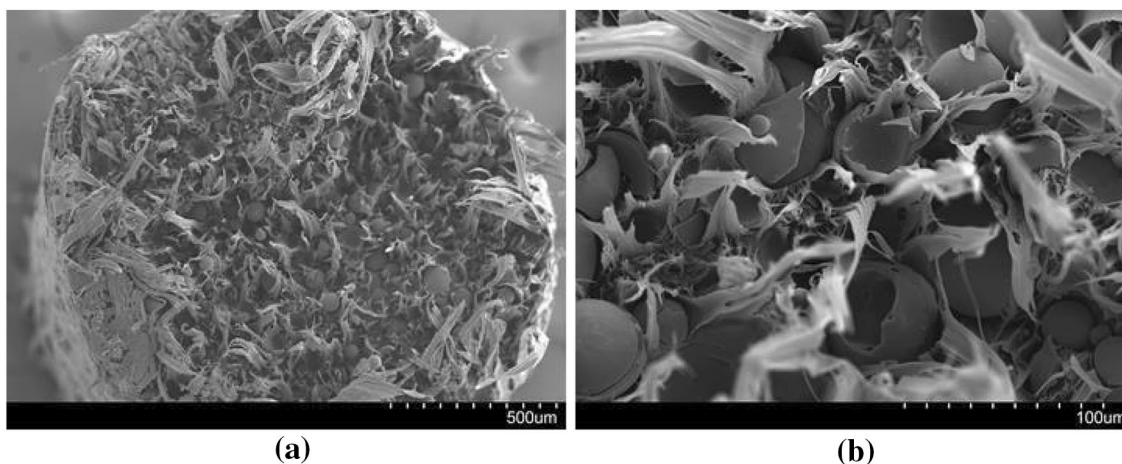


Fig. 4. Tensile fracture surface of HDPE40-2 \times filament tested at 10^{-4} s $^{-1}$ at (a) low and (b) higher magnifications.

specimens. Use of 60 vol.% less polymer and possibility of recycling make these filaments greener and more environmental friendly than the filaments of neat resin.

ACKNOWLEDGEMENTS

Mrityunjay Doddamani acknowledges the Department of Science and Technology, India, Grant DST/TSG/AMT/2015/394/G, and Visiting Scientist Fellowship Grant VSP 17-7-001 by the US Office of Naval research—Global (Program manager: Dr. Ramesh Kolar) to visit NYU for this work. Nikhil Gupta acknowledges the Office of Naval Research Grant N00014-10-1-0988. The views expressed in this article are those of authors, not of funding agencies.

REFERENCES

1. I. Gibson, D. Rosen, and B. Stucker, *Additive Manufacturing Technologies: 3D Printing, Rapid Prototyping, and Direct Digital Manufacturing* (New York: Springer, 2015), pp. 1–18.
2. M. Attaran, *Bus. Horiz.* 60, 677 (2017).
3. D.-A. Türk, F. Brenni, M. Zogg, and M. Meboldt, *Mater. Des.* 118, 256 (2017).
4. F. Chen, G. Mac, and N. Gupta, *Mater. Des.* 128, 182 (2017).
5. D. Cooper, J. Thornby, N. Blundell, R. Henrys, M.A. Williams, and G. Gibbons, *Mater. Des.* 69, 44 (2015).
6. F.P.W. Melchels, M.A.N. Domingos, T.J. Klein, J. Malda, P.J. Bartolo, and D.W. Huttmacher, *Prog. Polym. Sci.* 37, 1079 (2012).
7. W. Zhong, F. Li, Z. Zhang, L. Song, and Z. Li, *Mater. Sci. Eng. A* 301, 125 (2001).
8. M.L. Shofner, K. Lozano, F.J. Rodríguez-Macías, and E.V. Barrera, *J. Appl. Polym. Sci.* 89, 3081 (2003).
9. N. Gupta, S.E. Zeltmann, V.C. Shunmugasamy, and D. Pinisetty, *JOM* 66, 245 (2014).
10. N. Gupta, D. Pinisetty, and V.C. Shunmugasamy, *Book Reinforced Polymer Matrix Syntactic Foams: Effect of Nano and Micro-Scale Reinforcement*, (Springer, NJ: Springer Briefs in Materials, 2013), pp. 19–24.
11. B.R. Bharath Kumar, M. Doddamani, S.E. Zeltmann, N. Gupta, M.R. Ramesh, and S. Ramakrishna, *Mater. Des.* 2016, 414 (2016).
12. M.L. Jayavardhan, B.R. Bharath Kumar, M. Doddamani, A.K. Singh, S.E. Zeltmann, and N. Gupta, *Compos. B Eng.* 130, 119 (2017).
13. B.R. Bharath Kumar, M. Doddamani, S.E. Zeltmann, N. Gupta, M.R. Ramesh, and S. Ramakrishna, *Data Brief* 6, 933 (2016).
14. J.J.C. Picot, *Polym. Eng. Sci.* 24, 415 (1984).
15. S. Yin, R. Tuladhar, F. Shi, R. Shanks, M. Combe, and T. Collister, *Polym. Eng. Sci.* 55, 2899 (2015).